Micromosaic formation in laser-irradiated Si probed by picosecond time-resolved x-ray diffraction

Hiroaki Kishimura,* Hiroto Morishita, Yasuhisa H. Okano, Yoichiro Hironaka, Ken-ichi Kondo, and Kazutaka G. Nakamura†
Materials and Structures Laboratory, Tokyo Institute of Technology, 4259 Nagatsuta, Midori, Yokohama 226-8503, Japan

Toshiyuki Atou
Institute for Materials Research, Tohoku University, 2-1-1 Katahira, Aoba, Sendai 980-8577, Japan
(Received 7 August 2006; revised manuscript received 20 October 2006; published 14 December 2006)

The transient lattice behavior of single-crystal Si(111) under 300 ps laser irradiation has been observed by time-resolved x-ray diffraction. At first, the rocking curves of the laser-irradiated Si(111) have a higher-angle-shifted component. The higher-angle component is attributed to lattice compression, which is induced by laser ablation. The maximum lattice strain is estimated at 5.6%, which is larger than the Hugoniot elastic limit for Si(111). After 1000 ps, a broadening of the main peak was recorded. In addition, the rocking curve of a recovered sample is clearly broader than that of a pristine sample. Reciprocal space mapping for the recovered sample shows that the lattice spacing of the recovered sample does not change from that of the pristine sample, whereas lattice planes are misoriented. The results of time-resolved measurement and the assessment of the recovered sample indicate that mosaic blocks with inclined orientations are induced by laser-driven elastic compression and the subsequent pressure release, rather than plastic deformation.

DOI: 10.1103/PhysRevB.74.224301 PACS number(s): 78.47.+p, 62.50.+p, 61.10.Nz

I. INTRODUCTION

The interaction between materials and a laser beam has been extensively studied because of its many useful applications. Laser ablation has become the predominant technology for such applications as the deposition of thin metals and dielectric films, welding, and micromachining. The laser shock treatment of metals is known as laser peening, and it is applied to improving their mechanical properties.[1] However, the precise mechanisms of the laser-induced modification of materials are not yet completely understood because of the lack of a fundamental understanding of lattice deformation processes.

A real-time observation of lattice dynamics at microscopic resolution provides information on the deformation mechanisms under laser irradiation on materials. In particular, x rays are a sensitive probe that provides structural information on crystalline materials. It is noticeable that recent developments in ultrafast laser systems enable us to use a laser-plasma-based x-ray source. Time-resolved x-ray diffraction (TXRD) with laser-plasma based x rays is capable of directly observing structural changes with fine time resolution. Ultrafast laser-induced structural changes have been investigated for some materials using TXRD with a subpicosecond time resolution.[2–4] Although laser-induced compressions on Si,[5–11] Ge,[12] CdS,[13] and Cu (Refs. 5 and 14) have been performed using TXRD, only an elastic lattice response has been detected. In this paper, we report the observation of the lattice dynamics of pulsed-laser irradiated Si using picosecond TXRD and the assessment of the recovered sample. We then discuss deformation dynamics under laser irradiation.

II. EXPERIMENT

In this study, time-resolved measurements were made using a laser pump and an x-ray probe. The laser system used was a Ti:sapphire base terawatt laser system (B. M. Industries Co. Ltd., α10us) based on a chirp pulse amplification (CPA) technique. The laser system can produce pulses having energy of up to 600 mJ for a duration of 300 ps at a wavelength of 790 nm (E=1.6 eV), and a repetition rate of 10 Hz. This 300 ps pulse beam was divided into two beams by a beam splitter. One beam (25%) was used to irradiate a sample through an optical delay line as a pump beam, and the other (75%) was compressed to approximately 60 fs and used to irradiate a Cu tape target at 10^{17} W/cm^2 in a vacuum chamber for the generation of pulsed x rays (6 ps pulse width).

The generated pulsed x rays were extracted through a Be window (127 μm thick) and focused on a sample with a Johansson-type bend crystal. X-ray diffraction was performed on a characteristic $K\alpha_1$ line of Cu in a symmetric Bragg diffraction geometry. The x rays from the bend crystal were focused on a sample to cover an angular range of 2.8° centered around the Si(111) Bragg angles. The diffracted x rays were recorded with x-ray charge-coupled device (CCD) area image sensors (Hamamatsu Photonics Co.), which were LN_2-cooled and have 1024×1024 pixels of 25×25 μm^2. X rays were diffracted at the center of the laser-irradiated spot on the sample. An x-ray diffraction pattern was obtained by accumulating 1000 shots.

The samples used were Si(111) wafers of 525 μm thickness and 100 mm diameter. The laser energy density on the excitation target was 54 GW/cm^2 by focusing the laser beam into spot sizes of 0.88 mm diameter on the sample with a planoconvex lens (f=150). The sample was mounted on a motorized XY stage. The laser irradiation spot was moved for each laser shot to prevent irradiation on the same spot.

The recovered samples were evaluated by reciprocal space mapping (RSM) using x rays and scanning electron microscopy (SEM) operating at 15 kV. The RSM was performed using an x-ray diffractometer (Brucker Co., Ltd., D8

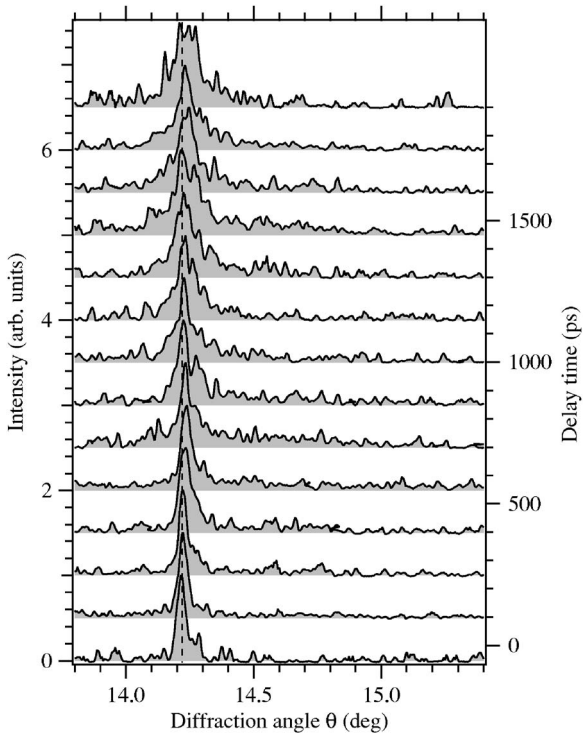

FIG. 1. Typical rocking curves for laser-irradiated Si(111) as functions of delay times. The delay time is varied from −50 to 1900 ps at 50 ps intervals. The dashed line shows the Bragg diffraction angle for the Cu $K\alpha_1$ line from the pristine Si(111). Higher-angle components appear at up to 1000 ps and the maximum shift is 0.81° at 700 ps. After 1000 ps, broad signals appear on both sides of the main peak, and the shape of the broad signal is independent of delay time.

Discover) with a Cu $K\alpha$ line. The probe x ray was collimated to about 100 μm diameter on the sample. The diffracted signals were recorded with a position-sensitive proportional counter. Reflections (333) and (331) were measured for recovered samples. The RSM was carried out at the center and off-center of the irradiated spot and in an unirradiated area.

III. RESULTS

A. Time-resolved x-ray diffraction

Figure 1 shows the rocking curves for 54 GW/cm^2 irradiation as functions of diffraction angle and delay time. The diffracted signal was measured in the (111) plane with the Bragg angle being 14.22°. The time delay $t=0$ is defined as the time when the lower-angle-or higher-angle-shifted component first appears. The delay time was varied from −50 to 1900 ps at 50 ps intervals. In Fig. 1, the profiles of the rocking curves are divided into two phases at 1000 ps. Before 1000 ps, the rocking curves of the laser-irradiated Si(111) have a higher-angle-shifted component, which indicates lattice compression. On the other hand, there are no signals at the lower angle. The broadening and intensity of the shifts become larger with delay time. The observed maximum shift is 0.81° at a delay time of 700 ps. In the symmetric Bragg diffraction configuration, the lattice strain can be

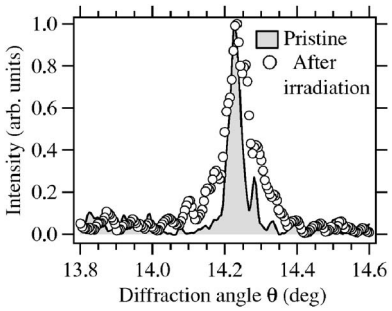

FIG. 2. Normalized rocking curves for Si(111) before and after laser irradiation. The FWHM of the rocking curve of the irradiated sample is larger than that of the pristine sample.

estimated using $\Delta d/d=-\Delta\theta\cot\theta_B$, where d is the lattice spacing, $\Delta\theta$ the shift, and θ_B the Bragg angle. The maximum lattice strain is estimated at 5.6% and is larger than the Hugoniot elastic limit (HEL) for Si(111),[15,16] which is the limitation of elastic compression. The width of the shift decreases with an increase in delay time to 1000 ps. After 1000 ps, the features of the rocking curves are different from those before 1000 ps. Broad signals appear on both sides of the main peak, and the profiles of the broad signals are independent of pump-probe delay time. The full-width at half-maximum (FWHM) of the rocking curves β after 1000 ps is $0.104\pm0.002°$.

The observed rocking curves are regarded as a projection of two-dimensional reciprocal lattice point (RLP) of the (111) reflection. The rocking curves are affected by a shape of the RLP. Lattice strain causes the RLP stretching along the scattering vector and the rocking curves have higher-or lower-angle shifted components. Tilting of the lattice plane is related to a change along the direction perpendicular to the scattering vector. Grain size reduction corresponds to expansion of the RLP. Both tilting and grain size reduction result in a broadening of the rocking curve. Therefore the rocking curves reflect these effects.

B. Recovered sample

1. Rocking curve

Figure 2 shows the normalized rocking curves of the recovered sample. The broadening of the peak was maintained even after the laser irradiation. The FWHMs of the rocking curves for the irradiated and pristine samples are 0.061 ± 0.007 and $0.035\pm0.001°$, respectively. The present results suggest that an irreversible lattice deformation takes place within 1 ns. This is different from the results of laser-shocked Ge.[12]

2. Reciprocal space mapping

An irreversible broadening of the diffraction peak was observed from the recovered sample. The x-ray diffraction pattern is affected by crystallographic imperfections such as crystallographic tilting to the surface normal and the residual lattice strain. Crystallographic tilting and residual strain cannot be independently measured by a conventional rocking

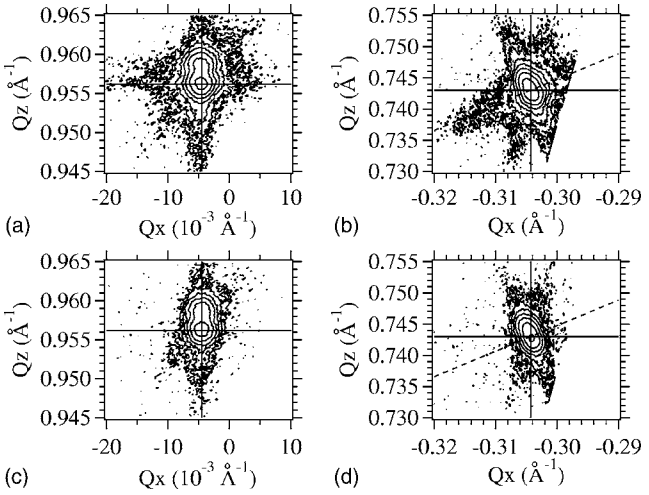

FIG. 3. RSM plots for recovered samples of (a) (333) and (b) (331) reflections and pristine samples of (c) (333) and (d) (331) reflections. The broken lines correspond to the minor axis of the elliptical shape. The centers of both samples are in good agreement. Broadening was clearly observed in the irradiated sample.

curve for a symmetric lattice plane because of the overlapping of these effects. RSM using x rays and an analytical method have been improved to evaluate the lateral grain size and character of the mosaic structure of a film having a large lattice mismatch.[17,18] The RSM gives us information about the character of a lattice plane. In reciprocal space, the broadening of reciprocal lattice points along the Qz-direction is related to variations in lattice spacing, whereas the broadening along the other axis is sensitive to tilts or twists of the lattice. The recovered samples were evaluated using RSM to explain the mechanism of the broadening of the rocking curve.

RSM plots for the recovered and pristine samples are shown in Fig. 3. The RSM plots show an elliptical shape. For each plot, the position of the centers of the ellipses along the Qz-direction are highly consistent with the lattice constant of the pristine sample. This indicates that the lattice constant of the recovered sample has not changed. In other words, plastic lattice deformation does not occur at the present laser power density. In contrast, broadenings along the Qx-axis [Fig. 3(a)] and minor axis [Fig. 3(b)] are clearly shown in the RSM plots for the recovered sample. The broadening of the RSM plots at the center of the irradiated spot was slightly larger than that measured off-center. The broadening is considered to be due to the characteristic features of mosaic block tilting.[17–20] The RSM results imply the formation of mosaic blocks with misoriented lattice planes caused by laser irradiation.

3. SEM images

SEM images of the laser-irradiated Si sample are shown in Fig. 4. Figure 4(a) shows the morphology at the center of the irradiated spot. It appears that sterically complicated features and complex cavities are formed. In Fig. 4(b), the surface has tubelike structures with small holes and spherical shapes. The diameters of the tubes are approximately 3 μm,

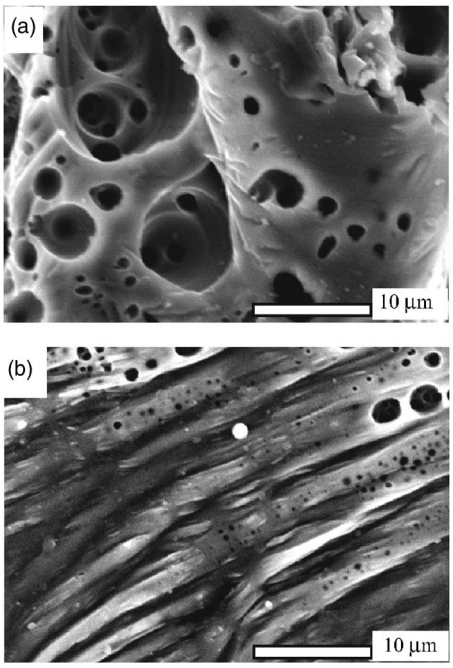

FIG. 4. Typical SEM images of laser-irradiated Si at (a) center and (b) off-center. Complex features are shown at the center.

but the directions of the tubes depend on their location. These structures suggest thermal melting and recrystallization caused by the laser irradiation. This surface morphology is similar to the results obtained by laser irradiation on poorly absorbed semiconductors.[21] The existence of cavities is understood to be caused by the vapor of a boiling layer inside the crystal being ejected from the cooled surface. Thus vaporization from the inner layer is presumed to occur at a later phase of laser irradiation.

IV. DISCUSSION

In this study, lattice compression was observed under laser irradiation. Although a thermoelastic response of Si heated by laser irradiation may occur,[22] the expected compression is approximately 0.2%, which is lower than the observed compression of 5.6%. In a laser shock experiment, the origin of uniaxial compression in a sample is thought to be laser ablation. The ablation pressure for this study is estimated to be 8.3–9.4 GPa.[23,24] The HEL is at a compression of 2.6%, corresponding to a dynamic pressure of 5.4 GPa.[15,16] The ablation pressure is greater than the HEL but is less than the pressure required for a semiconductor-metal transition of approximately 12 GPa.[25]

The FWHM of the peak during the laser irradiation ($\beta \sim 0.104°$) is larger than that of the recovered sample ($\beta \sim 0.061°$). It is speculated that the peak broadening after 1000 ps is not due to thermal effect because the broadening is detected in early stages. The narrowing of the peak indicates that the ordering of the crystal or regrowth of the crystal driven by residual heat may occur. SEM images show that the temperature inside the sample remains high after the surface layer has been cooled. Note that TXRD is not apprecia-

bly affected by surface morphology, which is observed by SEM. Because the penetration depth for Cu $K\alpha$ for an incident angle of 14.22° is 8.3 μm, TXRD gives information on the inner crystal. In contrast to TXRD, SEM can reveal only surface morphology. In addition, the penetration depth of Si for 790 nm light is about 10 μm, and it decreases with increasing temperature;[26] then a thin surface layer is melted and ablated. Consequently, the residual heat of the surface layer may diffuse into the inner crystal and the regrowth of the sample might be observed using TXRD.

The lattice compression induced by the laser ablation appears immediately after laser irradiation. SEM images indicate that heterogeneous boiling known as phase explosion[27] may occur and babbles are ejected from the surface. On the other hand, numerical simulation reveals that phase explosion dose not occur under picosecond irradiation because of gradual cooling by heat conduction.[28] In any event, these events are relatively slow processes in the laser irradiation and it seems that these processes including melting, vaporization, and recrystallization are not reflected in our time-resolved measurement. It is speculated that laser-induced plasma formation causes the lattice compression. In this study, the laser fluence exceeds the optical breakdown threshold of Si.[29]

The mosaic blocks are characterized using the results of RSM and TXRD. The lattice tilt distribution q is related to the deviation of the RSM ($\Delta\psi$).[19] The lattice tilt distribution is obtained using

$$\Delta q = 2K\Delta\psi \sin\theta_B, \tag{1}$$

where K is the wave vector of x rays. The RSM of the asymmetric reflection 331 for the irradiated sample gives a tilt distribution of $\Delta q = 0.071°$. The tilt angle is comparable with the FWHM of the rocking curves for the irradiated sample within experimental error. This implies that the irreversible broadening of the rocking curves is due to mosaic blocks tilting. The size of the grain can be estimated using Scherrer's equation

$$d_{mosaic} = \frac{0.9\lambda}{\beta\cos\theta_B}, \tag{2}$$

where λ is the wavelength of x rays. The estimated grain size is about 200±60 nm. However, the RSM clearly shows anisotropic broadening of the RLP. It is indicated that the broadening is caused by the tilt of lattice plane.

The residual stress of the Si crystal is expected to be applied during recrystallization processes. Raman spectra obtained using a 514.5 nm line of Ar laser show that both compressive and expansive stress of several hundreds MPa is applied in laser-irradiated Si.

Considering the results of TXRD and RSM, it is assumed that the formation of misoriented mosaic blocks is caused by laser irradiation. In fact, it has been reported that plastic deformation due to laser irradiation induces mosaic-block formation in metal.[30,31] In this study, however, although the duration of the laser pulse was only 300 ps, the broadening of the rocking curve was observed at a delay time of 1000 ps. In other words, laser-driven compression was terminated when the broadening was first observed. Moreover, taking the results of RSM into account, it is reasonable to assume that an imperfect plastic deformation is induced by laser-induced compression. This means that the formation of misoriented mosaic blocks is not only attributed to laser-induced compression. It has been reported that laser-shock compression in semiconductors shows a simple elastic response above the HEL.[5–12] In addition, elastic compression followed by elastic tensile strain has been reported. The obtained compression was 6.2±0.2% and the maximum tensile strain was 3.4%, which is comparable to the fracture stresses obtained in static measurement.[9] It is speculated that a large tensile strain causes a marked tilting of the lattice plane in the mosaic blocks.

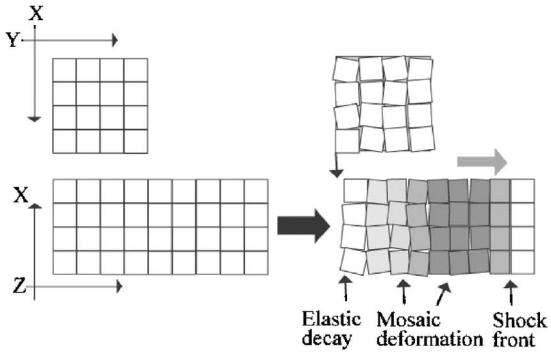

FIG. 5. Schematic drawing of lattice response under laser irradiation. The *XY*-plane corresponds to the (111) lattice plane, which is perpendicular to the incident beam. The sample is a perfect crystal before the laser irradiation. When the surface of the sample is laser-irradiated, lattice compression along the *Z*-direction occurs. Mosaic deformation with a slight tilt occurs simultaneously with the compression. The misorientation of the mosaic blocks is enhanced by the large tensile strain induced during relaxation.

A schematic drawing of the lattice response to the laser irradiation is shown in Fig. 5. In Fig. 5, the *XY*-plane corresponds to the (111) lattice plane and the *Z*-direction is the [111] direction. Before the laser irradiation, the sample is a perfect crystal. During the laser irradiation, laser ablation is induced and lattice compression occurs along the *Z*-direction. Because of the compression, mosaic blocks that are slightly tilted and twisted are formed. The spaces between the mosaic blocks are considered to be amorphous and the sizes of both spaces and mosaic blocks are decreased by the compression. After the laser irradiation has finished, pressure is released, and then a marked tilting of each block is induced by the large tensile stress due to the pressure release. Note that the scheme explains the deformation of the inner crystal but it cannot account for surface changes.

Previous studies of laser-induced shock compression in Si (Refs. 5–11) and Ge (Ref. 12) showed that the crystal response is purely elastic. In the case of Si(100), nanosecond shock experiments of up to 60 GPa were performed using an indirect (x-ray) or direct (laser) drive and the shocked crystal was probed by x-ray diffraction.[5,6] These results show that Si appears to respond elastically on the nanosecond time scale. In this study, the lattice response should be the same as those of previous studies. However, the RSM plots and the consid-

erable peak broadening imply that the lattice response to laser irradiation is not always simply elastic. A possible reason for this discrepancy is that the time and angle resolution of this study are better than those of previous studies.

V. CONCLUSION

Lattice compression in Si(111) induced by laser irradiation at 54 GW/cm^2 has been measured by time-resolved x-ray diffraction. The results indicate an elastic lattice compression during a 300 ps laser irradiation followed by irreversible deformation. Reciprocal mapping for recovered Si implies that mosaic blocks with various misoriented planes are formed. The irreversible deformation is concluded to be caused by elastic compression and the subsequent large tensile strain, rather than plastic compression.

ACKNOWLEDGMENTS

This study was supported in part by Grants-in-Aid for Scientific Research No. 14077209 (Scientific Research on Priority Areas) from the Ministry of Education, Culture, Sports, Science and Technology. The authors are grateful to the JSPS. The authors thank M. Hasegawa for his help in constructing the experimental setup. The authors thank Y. Horie of Air Force Research Laboratory for valuable discussions.

*Present address: Department of Materials Science and Engineering, National Defense Academy, Yokosuka, Kanagawa 239-8686, Japan.

†Author to whom correspondence should be addressed. Email address: nakamura.k.ai@m.titech.ac.jp

[1] C. S. Montross, T. Wei, L. Ye, G. Clark, and Y. Mai, Int. J. Fatigue **24**, 1021 (2002).

[2] C. W. Siders, A. Cavalleri, K. Sokolowski-Tinten, Cs. Toth, T. Guo, M. Kammler, M. Horn-von-Hoegen, K. R. Wilson, D. von der Linde, and C. P. J. Barty, Science **286**, 1340 (1999).

[3] A. Cavalleri, Cs. Toth, C. W. Siders, J. A. Squier, F. Raksi, P. Forget, and J. C. Kieffer, Phys. Rev. Lett. **87**, 237401 (2001).

[4] K. Sokolowski-Tinten, C. Blome, J. Blums, A. Cavalleri, C. Dietrich, A. Tarasevitch, I. Uschmann, E. Forster, M. Horn-von-Hoegen, and D. von der Linde, Nature (London) **422**, 287 (2003).

[5] A. Loveridge-Smith, A. Allen, J. Belak, T. Boehly, A. Hauer, B. Holian, D. Kalantar, G. Kyrala, R. W. Lee, P. Lomdahl, M. A. Meyers, D. Paisley, S. Pollaine, B. Remington, D. C. Swift, S. Weber, and J. S. Wark, Phys. Rev. Lett. **86**, 2349 (2001).

[6] D. H. Kalantar, J. Belak, E. Bringa, K. Budil, M. Caturla, J. Colvin, M. Kumar, K. T. Lorenz, R. E. Rudd, J. Stolken, A. M. Allen, K. Rosolankova, J. S. Wark, M. A. Meyers, and M. Schneider, Phys. Plasmas **10**, 1569 (2003).

[7] J. S. Wark, R. R. Whitlock, A. Hauer, J. E. Swain, and P. J. Solone, Phys. Rev. B **35**, 9391 (1987).

[8] J. S. Wark, R. R. Whitlock, A. A. Hauer, J. E. Swain, and P. J. Solone, Phys. Rev. B **40**, 5705 (1989).

[9] J. S. Wark, N. C. Woolsey, and R. R. Whitlock, Appl. Phys. Lett. **61**, 651 (1992).

[10] Y. Hironaka, A. Yazaki, F. Saito, K. G. Nakamura, K. Kondo, H. Takenaka, and M. Yoshida, Appl. Phys. Lett. **77**, 1967 (2000).

[11] H. Kishimura, A. Yazaki, Y. Hironaka, K. G. Nakamura, and K. Kondo, Appl. Surf. Sci. **207**, 314 (2003).

[12] K. G. Nakamura, H. Kawano, H. Kishimura, Y. Okano, Y. Hironaka, and K. Kondo, Jpn. J. Appl. Phys., Part 1 **43**, 5477 (2004).

[13] T. d'Almeida, M. D. Michiel, M. Kaiser, T. Buslaps, and A. Fanget, J. Appl. Phys. **92**, 1715 (2002).

[14] M. A. Meyers, F. Gregori, B. K. Kad, M. S. Schneider, D. H. Kalantar, B. A. Remington, G. Ravichandran, T. Boehly, and J. S. Wark, Acta Mater. **51**, 1211 (2003).

[15] W. H. Gust and E. B. Royce, J. Appl. Phys. **42**, 1897 (1971).

[16] T. Goto, T. Sato, and Y. Syono, Jpn. J. Appl. Phys., Part 2 **21**, L369 (1982).

[17] R. Chierchia, T. Bottcher, H. Heinke, S. Einfeldt, S. Figge, and D. Hommel, J. Appl. Phys. **93**, 8918 (2003).

[18] A. Ohtomo, H. Kimura, K. Saito, T. Makino, Y. Segawa, H. Koinuma, and M. Kawasaki, J. Cryst. Growth **214/215**, 284 (2000).

[19] K. Yokoyama, H. Kurihara, S. Takeda, M. Urakawa, K. Watanabe, M. Katou, N. Inoue, N. Miyamoto, Y. Tsusaka, Y. Kagoshima, and J. Matsui, Jpn. J. Appl. Phys., Part 1 **41**, 6094 (2002).

[20] K. Kondo, A. Sawaoka, and S. Saito, in *High-Pressure Science and Technology*, edited by K. D. Timmerhaus and M. S. Barber (Plenum, New York, 1979), Vol. 2, p. 905.

[21] V. Craciun and D. Craciun, Appl. Surf. Sci. **138-139**, 218 (1999).

[22] H. Kishimura, A. Yazaki, H. Kawano, Y. Hironaka, K. G. Nakamura, and K. Kondo, J. Chem. Phys. **117**, 10239 (2002).

[23] R. Fabbro, J. Fournier, P. Ballard, D. Devaux, and J. Virmont, J. Appl. Phys. **68**, 775 (1990).

[24] F. Dahmani, J. Appl. Phys. **74**, 622 (1993).

[25] A. Mujica, A. Rubio, A. Munoz, and R. J. Needs, Rev. Mod. Phys. **75**, 863 (2003).

[26] G. E. Jellison, Jr. and F. A. Modine, Appl. Phys. Lett. **41**, 180 (1982).

[27] J. H. Yoo, S. H. Jeong, X. L. Mao, R. Greif, and R. E. Russo, Appl. Phys. Lett. **76**, 783 (2000).

[28] P. Lorazo, L. J. Lewis, and M. Meunier, Phys. Rev. B **73**, 134108 (2006).

[29] P. P. Pronko, P. A. VanRompay, C. Horvath, F. Loesel, T. Juhasz, X. Liu, and G. Mourou, Phys. Rev. B **58**, 2387 (1998).

[30] P. Peralta, D. Swift, E. Loomis, C. H. Lim, and K. J. McClellan, Metall. Mater. Trans. A **36A**, 1459 (2005).

[31] H. Chen, Y. L. Yao, J. W. Kysar, I. C. Noyan, and Y. Wang, Int. J. Solids Struct. **42**, 3471 (2005).